OPEN JOURNAL SYSTEMS
ISSN:2237-2202

Available on line at Directory of Open Access Journals
Journal of Hyperspectral Remote Sensing v.11, n.1 (2021) 18-31

www.periodicos.ufpe.br/revistas/jhrs

Journal of Hyperspectral Remote Sensing
www.ufpe.br/jhrs

Obtaining the daily actual evapotranspiration through remote sensing techniques application in Brazilian Semiarid

Camilla K. Borges[*], Rayonil G. Carneiro[**], Cleber A. dos Santos[***], Carlos A. C. dos Santos[****]

[*]Universidade Federal de Campina Grande - UFCG, Campina Grande, Paraíba, Brasil.
E-mail: camillakassar@gmail.com (autor correspondente)
[**]Instituto Nacional de Pesquisas Espaciais - INPE, São José dos Campos, São Paulo, Brasil.
E-mail: rayonilcarneiro@gmail.com
[***]INPE, São José dos Campos, São Paulo, Brasil. E-mail: cleberassis.ufpa@gmail.com
[****]UFCG, Campina Grande, Paraíba, Brasil. E-mail: carlos.santos@ufcg.edu.br

Received 6 December 2020; accepted 20 May 2021

Abstract

Large volumes of water are released to the atmosphere through evaporation from soil and transpiration from vegetation, constituting evapotranspiration (*ET*). Estimating the water consumption in vegetated areas is important for the management and rational use of this resource. For this study were processed orbital images which correspond to Quixeré-CE, with interest at the Frutacor Farm, where there is predominance the banana crop. The main objective of this study was to assess the accuracy and applicability of S-SEBI and SSEB algorithms with regard to SEBAL to estimate the actual daily evapotranspiration (ET_a) of a semi-arid region of Northeast Brazil, containing areas of banana orchard, native vegetation (caatinga) and bare soil. S-SEBI. The SSEB and SSEB algorithms showed strong correlation ($r > 0.93$) with statistical significance of 5%. The S-SEBI exhibited errors less than 12% in the orchard and caatinga and SSEB exhibited greater errors at 22%, though for the bare soil, both models showed large discrepancies when compared with SEBAL, with errors greater than 36%. Therefore, among the two algorithms compared with SEBAL, S-SEBI had a better performance in ET_a estimation with lower deviations.
Keywords: Evapotranspiration, semiarid, SEBAL, S-SEBI, SSEB.

1. Introduction

Evapotranspiration is an important component of the hydrological cycle and one of the essential ecosystems processes for maintaining life on the planet. In addition, it is responsible for the release of large amounts of water from the surface to the atmosphere in steam form, occurring in a combined way by the evaporation of water bodies, soil and moist vegetation, together with the transpiration of the plants. Along with this, there is its contribution to the conversion of energy, moisture between the soil-vegetation-atmosphere and the regulation of the local and regional climate. It is influenced by biophysical, environmental and meteorological factors, such as precipitation, air and soil moisture, canopy conductance, leaf area, liquid radiation, air temperature, vapor pressure deficit, wind speed, etc. (Allen et al., 2007; Liou et al., 2014; Bezerra, 2015b; Sun et al, 2018).

In certain regions, evapotranspiration corresponds to more than half of the total precipitation, and in arid and semi-arid areas, this amount can be even greater than 90%, being decisive for freshwater recharging and groundwater discharging in these environments (Huxman et al. 2005; Yang et al., 2013; Liou et al., 2014). Hence, it is very important to estimate it more precisely, as well as to monitor its temporal and spatial distribution, in those areas that undergo prolonged periods of water scarcity and that tend to have highly variable precipitation and evapotranspiration, both spatially and temporally (Yang et al., 2013; Najmaddin et al., 2017).

The evapotranspiration determination is done by methods such as: lysimeters, Penman-Monteith, Bowen ratio, eddy covariance, orbital remote sensing, which allow its application in water resource management, irrigation planning, drought monitoring, climate forecasts, among others (Ruhoff et al., 2012; Liou et al., 2014; Bezerra et al., 2015a; Basit et al., 2018; Danodia et al., 2019). Due to the lack of specific meteorological and micrometeorological data from some locations, which makes it difficult to determine the surface energy fluxes, and consequently evapotranspiration. The application of remote sensing techniques that make it possible to analyze their variability in both spatial and temporal scale; It becomes advantageous as to logistics, technique, and budgetary. (Santos, 2009; Knipper et al, 2017).

The application of remote sensing techniques has the advantage of providing estimates on a regional scale, they do not produce errors due to instrument failures and facilitate the research in remote areas; different from field instruments (Liou et al., 2014). However, calibration must be considered, as it ensures the quality of the data generated by remotely located sensors, in addition to guaranteeing the possibility of converting the data recorded by the sensors into physical quantities correlated to the geophysical, chemical or biophysical parameters of objects (Ponzoni et al., 2015). They also have some limitations, when not applied on clear skies, since some sensors have a low temporal resolution, require subjective detection of the contrast between dry and wet areas in the image (Santos et al., 2010; 2011; Liou et al., 2014).

In relation to this problem of obtaining energy fluxes and evapotranspiration, several models have been developed from orbital remote sensing data, such as SEBAL (Surface Energy Balance Algorithm for Land), METRIC (Mapping Evapotranspiration at High Resolution with Internalized Calibration), SEBS (Surface Energy Balance System) (Bastiaanssen, 1995; Su, 2002; Jin et al., 2019). However, most of these models are based on the concept of energy balance and they are dependent on the time series of meteorological stations. Which does not happen with the S-SEBI (Simplified Surface Energy Balance Index), SSEB (Simplified Surface Energy Balance) models, since their estimates are obtained by the contrast between wet and dry areas in satellite images (Bezerra et al., 2015b; Knipper et al., 2017; Basit et al., 2018; Danodia et al., 2019).

Therefore, this study aims to understand the behavior and spatial variability of energy fluxes at the surface and the actual daily evapotranspiration, and thus verify the applicability and effectiveness of these estimates through the S-SEBI and SSEB models, in relation to the SEBAL model, which has already been tested and validated in several locations, and which in this survey was applied for different land uses: agricultural areas (banana orchard with homogeneous soil coverage); native vegetation (Caatinga, with heterogeneous soil cover) and bare soil, based on orbital images of Landsat 5 - TM from Quixeré - CE. In addition to obtaining the evapotranspiration by FAO - 56 method (Allen et al, 1998), in order to validate the two studied algorithms.

2. Material and methods

Study area

The studied area was located at the Frutacor farm (coordinates: 5º08'44"S, 38º05'53" W), in Quixeré - CE municipality (Figure 1), in the micro-region of Lower Jaguaribe River, with an average elevation of 147 m, approximately 250 ha of Pacovan banana cultivation, in addition to areas of native vegetation (Caatinga) and bare soil. The place has a dry and hot semi-arid climate, according to the Koppen – Geiger classification (Dubreuil et al., 2018) is BSh type, with an average annual temperature of 28.5 ºC and temperature ranging from 22 to 36ºC. The average annual precipitation for a period of 39 years (1974 - 2013) was 709.18 mm, from observations recorded by *Fundação Cearense de Meteorologia* (FUNCEME) at Quixeré - CE weather station, being the annual average of the relative humidity is 62%.

Data

For this study were processed data from Thematic Mapper (TM) sensor on board Landsat 5 satellite, from 10/24/2005 and 08/08/2006, which correspond to the days of the year (DOY), 297 and 220, from orbit 16 and point 64. It was used products obtained from the SEBAL methodology, derived from Santos (2009) study, in which they served as parameters for the comparison and verification of the applicability of the S-SEBI and SSEB models, through clippings of interest areas: bananas orchard, native vegetation (Caatinga) and bare soil. These models were applied to estimate the fluxes of sensible heat (*H*), latent heat (*LE*), soil heat (*G*), evaporative fraction (Λ), evapotranspiration fraction (ET_f) and daily actual evapotranspiration (ET_a).

Surface Energy Balance Algorithm for Land (SEBAL)

The SEBAL model is based on the concept of energy balance (*BE*), which relates the net radiation at the surface, called net radiation (R_n), converted into latent heat flux (*LE*), sensible heat flux (*H*) and soil heat flux (*G*) (Aguiar et al., 2018).

$$R_n - G \approx H + LE \qquad (1)$$

The processing of R_n process follows the methodology described by Allen et al. (2002), through the calculations of spectral radiance (L_λ), monochromatic reflectance (ρ_λ), albedo (α), vegetation indices, such as the Normalized Difference Vegetation Index (NDVI), Soil Adjusted Vegetation Index (SAVI), Leaf Area Index (LAI), surface temperature (T_s), outgoing longwave radiation ($R_{L\uparrow}$), incoming longwave radiation ($R_{L\downarrow}$) and incoming shortwave radiation ($R_{S\downarrow}$).

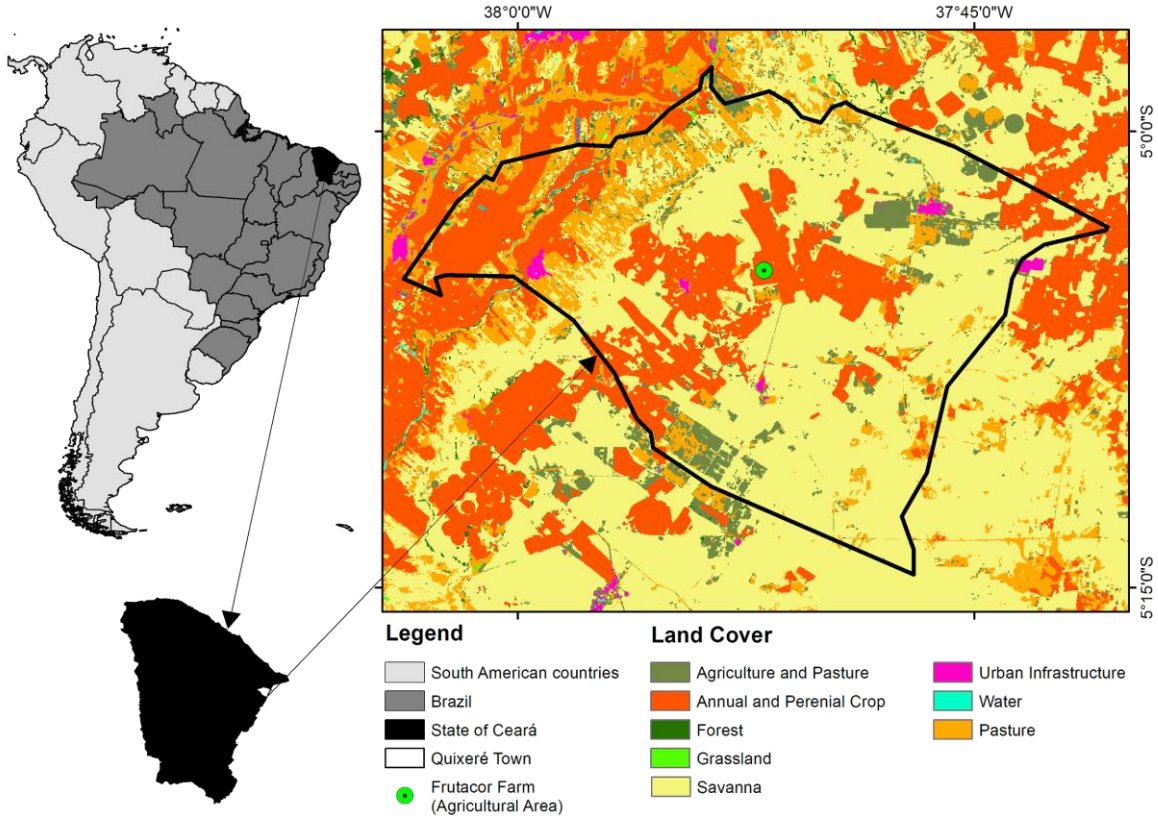

Figure 1 - Brazil map with an emphasis for Quixeré municipality in Ceará state; and the different land cover.

The computation of the physical quantities described above, and the surface thermal emissivity (ε_0) to obtain R_n, with unit of W m^{-2}, given by the following equation:

$$R_n = (1-\alpha)R_{S\downarrow} + R_{L\downarrow} - R_{L\uparrow} - (1-\varepsilon_0)R_{L\downarrow} \quad (2)$$

Whereas, the heating air rate, namely, the sensible heat flux (H) is a function of the surface roughness, wind speed, and air temperature difference between two levels close to the surface (ΔT) (Silva et al., 2018),

$$H = \frac{\rho c_p \Delta T}{r_{ah}} \quad (3)$$

where, ρ is the humid air density (kg m^{-3}), c_p is the specific dry air heat at constant pressure (1004 Jkg^{-1}K^{-1}) and r_{ah} is the aerodynamic resistance (s m^{-1}).

Wherein, H was obtained by the linear relationship between T_s and ΔT, and it was given by the linear equation coefficients, which they obtained from the selection of the "anchor pixels", where one is the hot pixel and the other is the cold pixel. The temperature difference of a dry surface (hot pixel) is found considering the $LE = 0$ when all the available power (R_n - G) is converted into H. At the wet surface (cold pixel), almost all (R_n - G) is used for the evaporation process, consequently $H = 0$ and $\Delta T = 0$ (Bastiaanssen et al., 1998a; 1998b; Calcagno et al., 2007; Jia et al., 2013; Silva et al., 2018).

The soil heat flux (G) was calculated from the description by Bastiaanssen (2000):

$$G = \left[\frac{T_s}{\alpha}\left(0{,}0038\alpha + 0{,}0074\alpha^2\right)\left(1 - 0{,}98IVDN^4\right)\right]R_n \quad (4)$$

From equation (1), LE is provided by subtracting H from (Rn-G), such that LE is calculated as a residue of BE, as described by Bastiaanssen et al. (1998a), Weligepolage (2005) and Santos (2009). Thus, through the results obtained by SEBAL processing steps, ETa was estimated from LE (Bastiaanssen et al., 1998a; Jia et al., 2013).

Daily actual Evapotranspiration (ET_a)

The hourly actual evapotranspiration (ET_h) given in *mm/h* is estimated from the SEBAL and S-SEBI algorithms, whose equation is a function of the latent heat flux density LE,

$$ET_h = 3600\,LE/L \quad (5)$$

such that, L is the latent heat of water vaporization (L = 2.45 x 106 J kg-1) and 3600 the conversion factor of instantaneous values of LE image to hourly values (Allen et al., 2002).

The ratio between *ETh* and hourly reference evapotranspiration (ET_{0_h}) is called the hourly evapotranspiration fraction (FET_{0_h}), which is calculated using the FAO / Penman-Monteith method proposed by Allen et al. (1998).

$$FET_{0\_h} = \frac{ET_h}{ET_{0\_h}} \quad (6)$$

Since the behavior of FET_{0_h} is almost constant during the day, it can be assumed that $FET_{0\_h} \simeq FET_{0\_24}$, where FET_{0_24} is the daily reference evapotranspiration fraction (Trezza, 2002; Santos, 2009). Therefore, the ET_a in *mm/day* is proportional to the daily reference evapotranspiration (ET_{0_24}):

$$ET_a = FET_{0\_h} . ET_{0\_24} \quad (7)$$

Simplified Surface Energy Balance Index (S-SEBI)

This is a more simplified methodology model developed by Roerink et al. (2000, when compared to SEBAL and METRIC for example, to estimate energy fluxes at the surface, based on the contrast between dry and wet surface conditions, detected by the relationship between albedo (α) and surface temperature (T_S) (Zahira et al., 2009; Basit et al., 2018; Danodia et al., 2019). To calculate the *LE* and *H* fluxes, the evaporative fraction has been obtained previously, as follows:

$$\Lambda = \frac{T_H - T_S}{T_H - T_{LE}} \quad (8)$$

where, T_H and T_{LE} are the temperatures corresponding to the contrasts (dry and wet) for a given albedo value, such that T_H is associated with the maximum *H* (minimum *LE*) and T_{LE} indicates the maximum *LE* (minimum *H*). These are derived from the linear regression between T_S and α, with the selection of rising and descending straight lines of the scatter plot in Figure 2 (Santos and Silva, 2008).

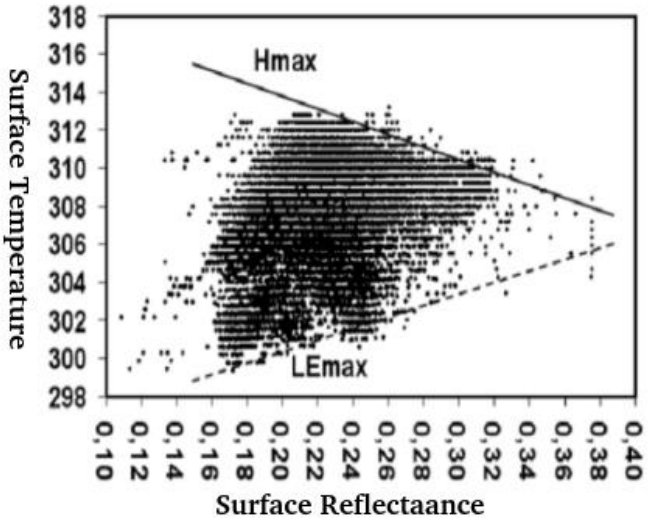

Figure 2 - Schematic representation of the scatterplot of surface temperature and surface reflectance (Source: Santos et al., 2010).

Linear regression is applied to the scatter points between the TH and TLE straight lines to obtain the equations that represent the maximum and minimum limits:

$$T_H = a_H + b_H \alpha_0 \quad (9)$$

$$T_{LE} = a_{LE} + b_{LE} \alpha_0 \quad (10)$$

where *a* and *b* are the regression coefficients and replacing equations (9) and (10) in (8), Λ is obtained, then the LE and H fluxes are calculated (Zahira et al., 2009).

$$H = (1 - \Lambda)(R_n - G) \quad (11)$$

$$LE = \Lambda(R_n - G) \quad (12)$$

wherein LE was used in equation (5) of the ET_a and the *G* calculation appears in equation (4).

Simplified Surface Energy Balance (SSEB)

The ET_a through the SSEB model, such that the evapotranspiration fraction (ET_f) is determined as described by Senay et al. (2007), wherein three anchor pixels are selected from the images of T_s and NDVI. The NDVI image serves as a guide for selecting areas of dry soil without vegetation cover, which refers to hot pixels, and areas of soil with dense vegetation cover and good soil water supply, for cold pixels. Which are identified by the combination of high T_s values and low NDVI values for hot pixels, and the opposite for cold pixels (Senay et al., 2007; 2011b).

The ET_f values range from 0 to 1, with the hot pixel being associated with the minimum *ET* and the maximum *ET* being associated with the cold pixel, and thus they represent differences in water availability and vegetation condition (Cai and Sharma, 2009; Senay et al., 2011b; Bezerra et al., 2015b).

$$ET_f = \frac{(T_H - T_s)}{(T_H - T_c)} \qquad (13)$$

With T_H being the average of the 3 hot pixels and T_c being the average of the 3 cold pixels selected based on the images of *NDVI* and T_s which is the input image of equation (13), generated through the calculations of R_n (Senay et al., 2007 ; Cai and Sharma, 2010).

Finally, the ET_a (mm / day) of a given scene is determined by ET_f and the reference evapotranspiration (ET_o), according to FAO / Penman-Montheith de Allen et al. (1998):

$$ET_a = ET_f . ET_0 \qquad (14)$$

Statistical Analysis

Percent Error

To compare the value of the estimated variables (V_{est}) by the S-SEBI and SSEB models in comparison to the reference value (V_{ref}) provided by SEBA;, the percentage error calculation was used with the following expression:

$$E_{\%} = \frac{|V_{est} - V_{ref}|}{V_{ref}} \times 100 \qquad (15)$$

Student *t* test

One of the most used distributions for small samples is the *t*-Student parametric test, which is widely applied in meteorological studies (Kousky and Kayano, 1994; Kayano and Kousky, 1996; Castro, 2002; Silva et al., 2013). It allows assessment of statistical differences between two samples, and it is applied to verify whether the average of distinct samples can be considered different at a given significance level (Blain, 2009; Huang and Paes, 2009).

The simple correlation analysis that measures the degree of relationship between the variables is given through the correlation coefficient (*r*) for sample data, which can also be tested statistically using the *t* - Student test. For the correlation significance test, the null hypothesis of interest (H_0) was considered when the population correlation is zero ($\rho = 0$) and the alternative hypothesis (H_1) is different from zero, according to a level of significance (α) stipulated. If H_0 is rejected, it is concluded that there is a significant relationship between the variables (Kazmier, 1982).

3. Results and discussion

Energy fluxes to the surface (H and LE)

The results obtained by the S-SEBI and SSEB models were compared with the SEBAL calculations taken as a reference, since they were validated by Santos (2009) for the same study region and elsewhere (Santos et al. 2010; 2011; Bezerra et al., 2015b; Silva et al., 2018).

The *LE* calculated for the banana orchard area (Table 1) showed percentage errors below 10%, while *H* exhibited approximated errors of 27 and 55%. In the Caatinga area (Table 2), the *LE* errors showed values less than 13% and H were less than 11%, demonstrating that there was little distinction between the S-SEBI estimations in relation to SEBAL in this location. For bare soil (Table 3), *LE* showed errors greater than 35%, while the *H* errors were 7 and 30%. The *H* flux had a great distinction between the errors in the orchard and the bare soil areas.

Table 1 - Percentage errors of *LE* and *H* fluxes estimated by the S-SEBI for the banana orchard compared to SEBAL.

DOA	*LE* (W/m^2)		Error (%)	*H* (W/m^2)		Error (%)
	SEBAL	S-SEBI		SEBAL	S-SEBI	
297 (2005)	484,7	437,1	9,8	87,3	135,0	54,6
220 (2006)	402,3	439,0	9,1	136,3	99,6	26,9

Table 2 - Percentage errors of *LE* and *H* fluxes estimated by the S-SEBI for Caatinga compared to SEBAL.

DOA	*LE* (W/m^2)		Error (%)	*H* (W/m^2)		Error (%)
	SEBAL	S-SEBI		SEBAL	S-SEBI	
297 (2005)	245,4	215,7	12,1	272,6	302,3	10,9
220 (2006)	467,6	475,8	1,8	87,4	79,2	9,4

Table 3 - Percentage errors of *LE* and *H* fluxes estimated by the S-SEBI for bare soil compared to SEBAL.

DOA	*LE* (W/m^2)		Error (%)	*H* (W/m^2)		Error (%)
	SEBAL	S-SEBI		SEBAL	S-SEBI	
297 (2005)	59,4	86,9	46,3	399,5	372,0	6,9
220 (2006)	230,6	314,8	36,5	284,4	200,3	29,6

The distinctions found in the percentage errors of LE and H, mainly H, it must be related to the differences in the methodologies for obtaining the S-SEBI and SEBAL fluxes, since SEBAL makes more elaborate calculations, with regard to physical-mathematical formalism to obtain H. In S-SEBI, the fluxes are not calculated as separated parameters, as in SEBAL, but through the evaporative fraction (Λ), which in turn is parameterized through each image. Whereas, in SEBAL, H is obtained through an iterative computational process, in order to identify the condition of atmosphere stability, and to make corrections in the aerodynamic resistance values to heat transport (Sobrino et al., 2005; Weligepolage, 2005; Santos, 2009; Santos et al., 2010; Mendonça et al., 2012).

Relationship between the Evaporative Fraction (Λ) *and the evapotranspiration fraction* (ET_f) *with the Normalized Difference Vegetation Index* (NDVI)

The processed images, composed of areas of vegetated soil (Caatinga and agriculture) and bare soil, whose parameters and Λ were obtained dispersion plots (Figure 3) and the simple linear regression with its coefficients (intercept and slope) and the determination coefficients (R^2), since the NDVI has seasonal variation similar to evapotranspiration and comprises one of the main parameters to estimate it. It was found that R^2 equal to 0.57 and 0.53 for days 297 (2005) and 220 (2006), in addition to verifying the growing behavior of Λ - SEBAL with NDVI, given the positives slopes values (1.19 and 0.94), showing a similar pattern by the description given by Wang and Cribb (2006), of a general increase in the fraction Λ with the NDVI for the Southern Great Plains region of the United States, as well as the study by Yebra et al. (2013) in 16 experimental sites of the FLUXNET network with different soil cover (perennial and deciduous forests, savanna, pasture, etc.).

Senay et al. (2011a) described some evapotranspiration fraction values greater than 0.80 for NDVI below 0.30, which was attributed to cloudiness by reducing the IVDN values, which leads the cooling of surface temperature, and thus increasing the fraction values (see equations 8 and 13). This behavior also was observed in data from Λ with NDVI, (Figure 3), which was possibly associated with the presence of clouds in the processed image.

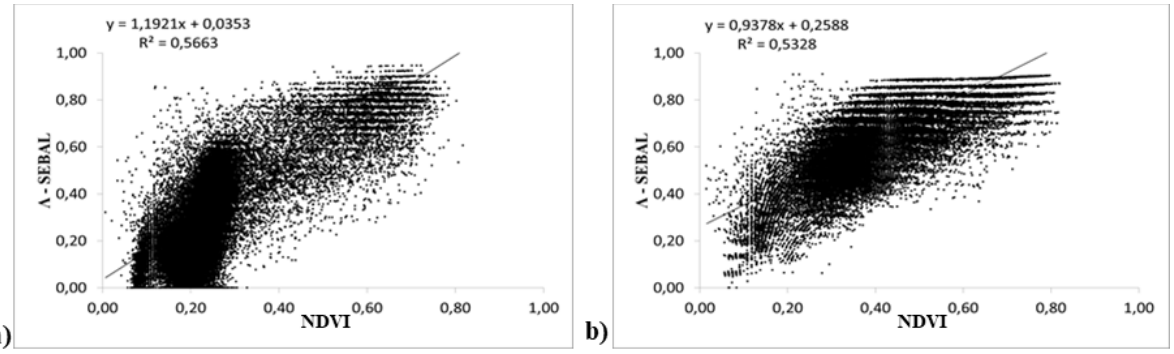

Figure 3 - Correlation between NDVI and the evaporative fraction (Λ) calculated by SEBAL, from the days 297/2005 (a) and 220/2006 (b).

From the comparison between the fractions with the NDVI (Table 4), they showed an increasing trend, with R^2 higher than 0.50, showing that the correlations (r) were higher than 0.70. Platonov et al. (2008) compared NDVI and ET_f values yielded through SSEB, which showed R^2 values ranging from 0.65 to 0.85 for a combination of the 3 images in the region of Syrdarya river basin in Central Asia. The lower values of R^2 were assigned to the influence of uncovered soil (bare soil) in the evapotranspiration process since the evaporation process is dominant as opposed to transpiration. The observation may be used to explain the occurrence of R^2 below 0.60 in the comparisons between Λ and ET_f with NDVI in this study since the scenes analyzed contained different types of ground cover.

Table 4 - Determination coefficients (R^2) of Λ and ET_f with NDVI and the corresponding equations of the linear regressions (y).

DOA	ET_f - SEBAL/NDVI		ET_f - S-SEBI/NDVI		ET_f - SSEB/NDVI	
	R^2	y	R^2	y	R^2	y
297 (2005)	0,57	1,19x+0,04	0,62	1,01x+0,09	0,65	1,19x-0,02
220 (2006)	0,53	0,94x+0,26	0,54	0,55x+0,50	0,56	1,16x+0,12

Through clippings from the days 297 (2005) and 220 (2006) from the Λ, the areas of the banana orchard, Caatinga and bare soil, that they were generated from the SEBAL and S-SEBI methods (Table 5), which were obtained R^2 greater than 0.75 ($r \geq 0.87$), with unexplained variation between models ranging from 24 to 2%, indicating the good fit and strong correlation between them. From the Λ averages, the *t - Student* was applied to determine the statistical significance of the correlation coefficients and the significance level at 5% ($\alpha = 0.05$). It was observed that there was a significant relationship between the Λ estimated from the S-SEBI algorithm in relation to SEBAL. In the study carried out by Zahira et al. (2009) found a determination coefficient of 0.61 for forest areas in western Algeria through the SEBAL and S-SEBI.

Table 5 - Determination coefficients (R^2) of the S-SEBI with the SEBAL for different land covers.

DOA	Orchard	Caatinga	Bare Soil
297 (2005)	0,76*	0,98*	0,95*
220 (2006)	0,98*	0,93*	0,78*

*significance level (α) of 5%.

From the values extracted from the Λ images, the averages and percentage errors of the tested algorithm S-SEBI having SEBAL as a reference (Table 6). In which, the averages in the orchard area were between 0.85 and 0.74. In the study by Bezerra et al. (2015a) in a cotton-growing area, in the Chapada do Apodi region in Northeast Brazil, the Λ ranged from 0.68 to 0.87 throughout the development of the crop; indicating coherence between the Λ values found in this study.

Table 6 - Evaporative fraction **(**Λ) estimated by SEBAL, S-SEBI models, for the orchard, Caatinga and bare soil areas, and their respective errors.

DOA	Λ – Orchard		Error	Λ – Caatinga		Error	Λ – Bare Soil		Error
	SEBAL	S-SEBI	(%)	SEBAL	S-SEBI	(%)	SEBAL	S-SEBI	(%)
297/2005	0,85	0,76	9,8	0,47	0,42	12,1	0,13	0,19	46,7
220/2006	0,74	0,81	9,2	0,84	0,86	1,8	0,45	0,61	36,6

It was also found that the errors were less than 13% for the areas of the orchard and the Caatinga, showing that the S-SEBI did not present great distinctions with SEBAL. Comparing the estimates of the bare soil area, greater discrepancies between the methods were noted, with errors greater than 35%, which may be associated with the inefficiency of the application of this algorithm in areas without vegetation cover and consequently with low moisture content in the soil. However, in general, day 220 (2006) exhibited the lowest values of errors, a fact that is possibly related to the moisture stored in the soil during the rainy season, since these models are efficient for detecting fluxes in locations that have a good water supply in the soil (Senay et al., 2011a; b).

Actual Evapotranspiration (ET_a)

The spatial distribution of the ET_a for the 297(2005) (Figure 4), as the final product of the SEBAL, S-SEBI and SSEB models, with emphasis on the banana orchard area (black square), in which they show high values of ET_a > 6.0 mm / day in white, indicating a greater transfer of water vapor from the surface to the atmosphere. The areas in medium gray tones present intermediate values, likely denoting the presence of native vegetation. Whereas, the dark gray to black colors (ET_a < 3.0 mm / day) show the bare soil areas, with minimum ET_a values. It was observed match in the spatial distribution pattern of ET_a calculated by the SEBAL model was greater with the S-SEBI (Figure 4b), than with the SSEB (Figure 4c), which showed a few lower level of accuracy than the S-SEBI for characterization the areas with the highest evapotranspiration.

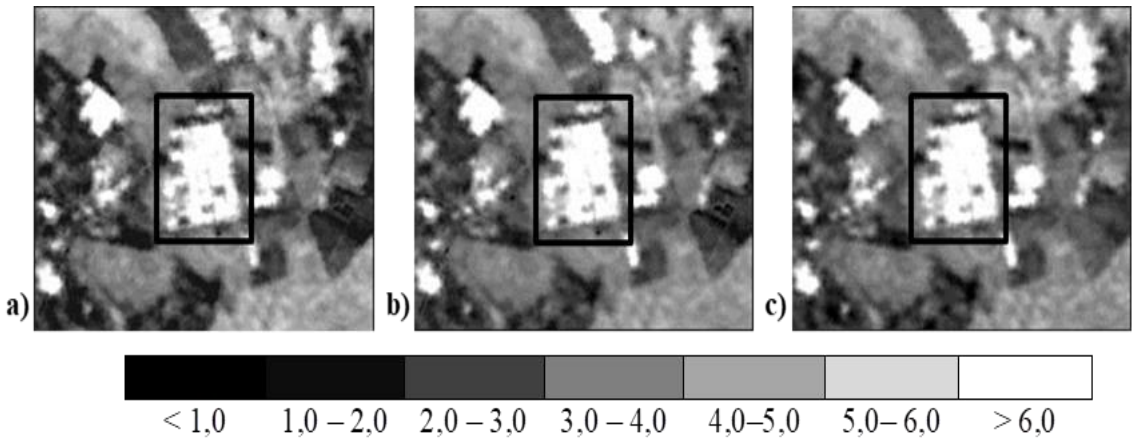

Figure 4 - ET_a spatial distribution (mm/day) for the day 297 (2005) through the models: SEBAL (**a**), S-SEBI (**b**), SSEB (**c**).

Figure 5 was similar to the previous analysis, the spatial distribution of ET_a for day 220 (2006); the S-SEBI model (Figure 5b) showed fewer discrepancies in relation to SEBAL. However, both S-SEBI and SSEB (Figures 4 and 5) demonstrated to underestimate ET_a, as it might be seen by the quality (definition) of these images when compared to the images generated by SEBAL.

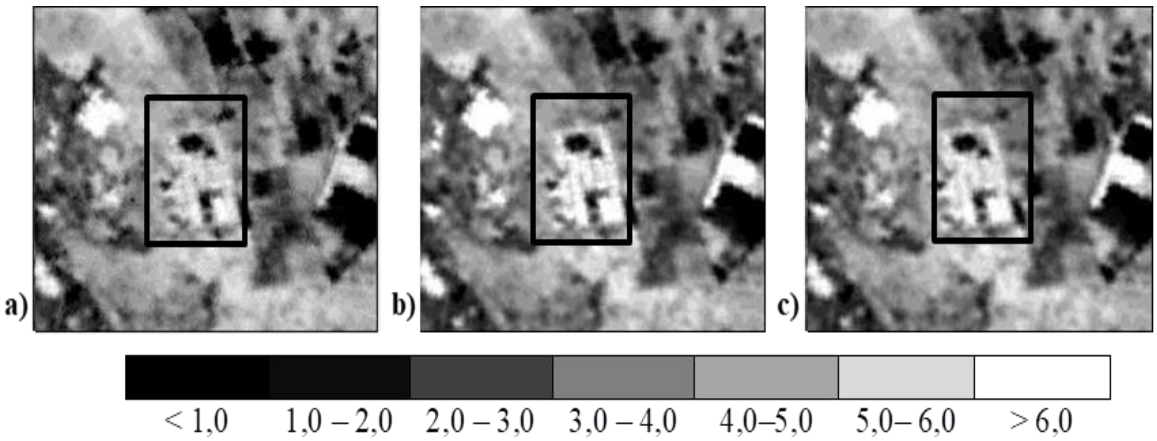

Figure 5 - ET_a spatial distribution (mm/day) for the day 220 (2006) through the models: SEBAL (**a**), S-SEBI (**b**), SSEB (**c**).

Figure 6 shows the ET_a correlations estimated by the S-SEBI and SSEB algorithms in relation to SEBAL, for the banana orchard area, whose correlations were quite satisfactory, greater than or equal to 0.89 ($R^2 \geq 0.79$). The dispersions in Figures 6a, 6b and 6d show that S-SEBI and SSEB underestimated ET_a, while in Figure 6c the S-SEBI overestimated. Similar behaviors were presented in the Caatinga area (Figure 7), with R^2 above 0.90 (r > 0.96), indicating a very good fit, with less than 10% of unexplained variation. In the correlations for the exposed soil, in Figure 8, the lowest R^2 value found was approximately 0.86, with r > 0.90 indicating a strong correlation and the good quality of the fit, since the explained variation of models was over 80%; it is indicative to predict them very well.

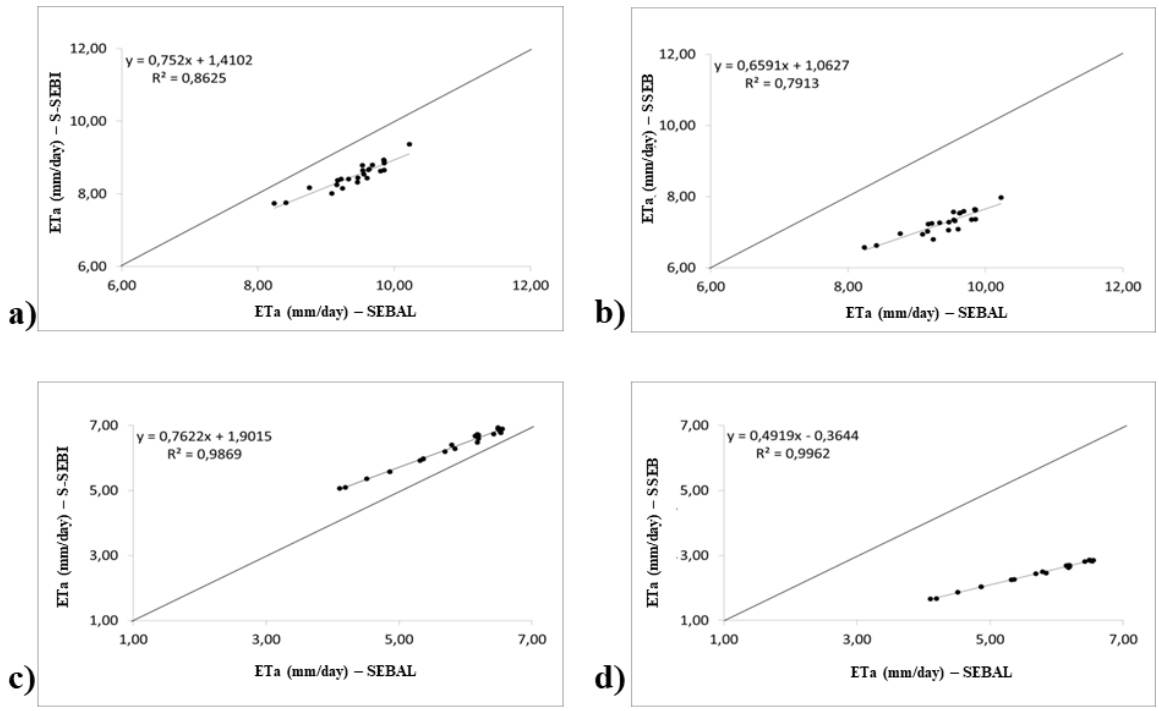

Figure 6 - Correlations between the ET_a estimated by SEBAL with the S-SEBI and SSEB for the banana orchard clippings on days 297 (a, b) and 220 (c, d).

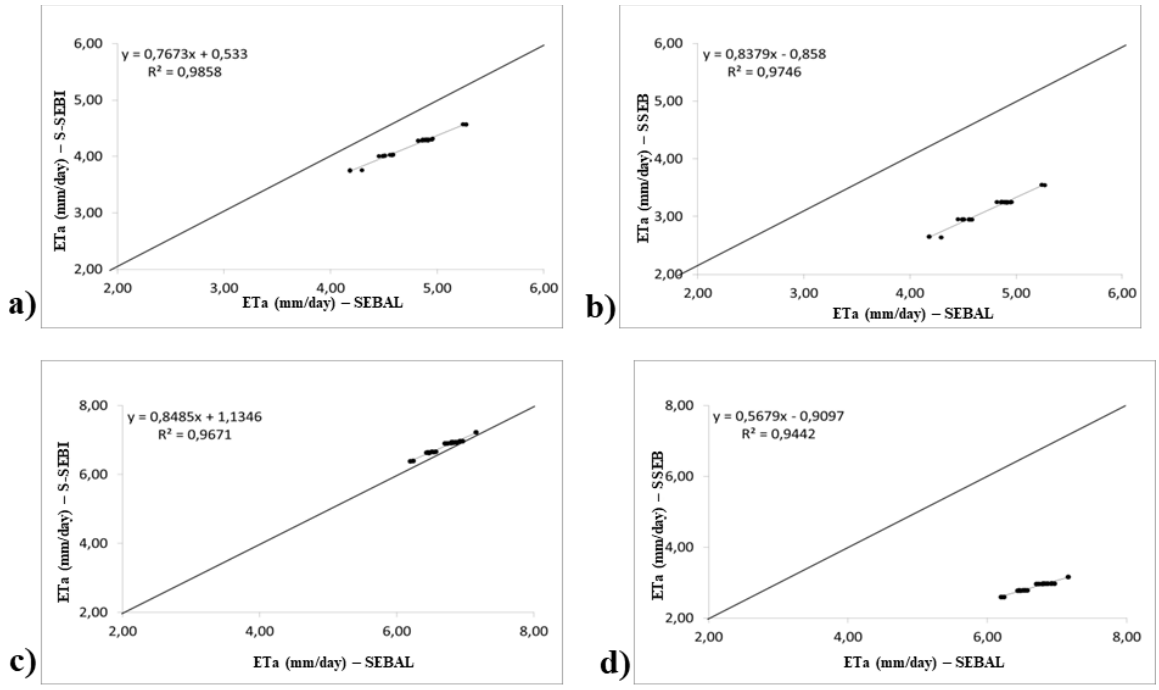

Figure 7 - Correlations between the ET_a estimated by SEBAL with the S-SEBI and SSEB for Caatinga clippings on days 297 (a, b) and 220 (c, d).

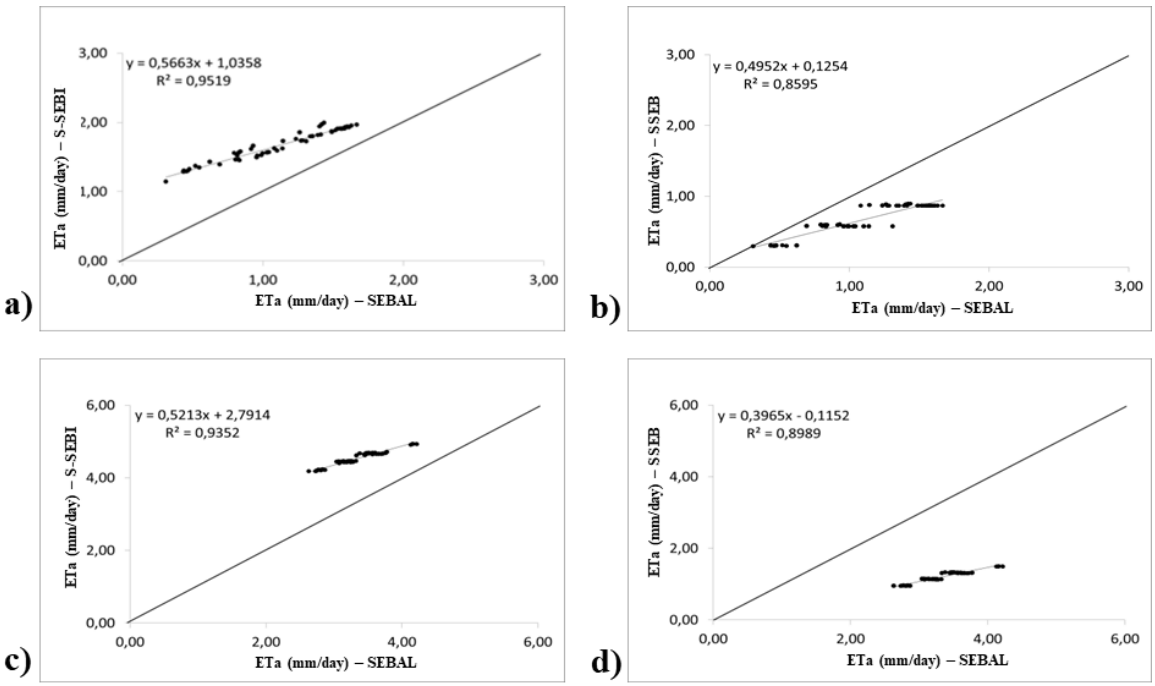

Figure 8 - Correlations between the ET_a estimated by SEBAL with the S-SEBI and SSEB for bare soil clippings on days 297 (a, b) and 220 (c, d).

It may be noted that the S-SEBI and SSEB models showed that they were quite satisfactory, that is, they were adequately predicted when compared with SEBAL since most of the variables exhibited R^2 greater than 0.85. Weligepolage (2005) found a strong correlation of daily ET_a ($R^2 = 0.95$), Santos et al. (2010) also found r equal to 0.85 (with a 5% statistical significance level). However, Senay et al. (2007) found r from 0.55 to 0.79, when comparing SSEB with SEBAL, which varied according to the type of culture.

The ET_a images obtained by the S-SEBI and SSEB algorithms were exported to spreadsheets, in which the averages and percentage errors were determined for the three types of areas assessed, taking SEBAL as a reference, according to Tables 7, 8, and 9. In the orchard area (Table 7), the S-SEBI showed errors of less than 10%, while the SSEB showed a much greater difference, with over errors than 21%. For the Caatinga (Table 8), just as in the orchard, S-SEBI showed less distinction, with errors below 13%, whereas the SSEB exhibited errors above 34%. Table 9, for the bare soil area, both models showed great distinction to SEBAL, with errors greater than 35%. From the average values of ET_a estimated by the three presented methodologies, the *t - Student* statistical test was applied, for $\alpha = 0.05$ and it was found that the null hypothesis for the equal population's averages was rejected. Thus, it could be inferred that there was a significant statistical relationship between the ET_a estimated by the models.

Table 7 - Actual evapotranspiration (ET_a) in mm / day estimated by the SEBAL, S-SEBI and SSEB models, for the banana orchard, and the respective percentage errors.

DOA	*ETa*– Orchard			Error (%) – SEBAL/S-SEBI	Error (%) – SEBAL/SSEB
	SEBAL	S-SEBI	SSEB		
297	9,4*	8,5*	7,3*	9,6	22,3
220	5,8*	6,3*	2,5*	8,6	57,0

*significance level (α) of 5%.

Table 8 - Actual evapotranspiration (ET_a) in mm / day estimated by the SEBAL, S-SEBI and SSEB models, for Caatinga, and the respective percentage errors.

DOA	*ETa*– Caatinga			Error (%) – SEBAL/S-SEBI	Error (%) – SEBAL/SSEB
	SEBAL	S-SEBI	SSEB		
297	4,8*	4,2*	3,1*	12,5	35,4
220/	6,7*	6,8*	2,9*	1,5	56,7

*significance level (α) of 5%.

Table 9 - Actual evapotranspiration (ET_a) in mm / day estimated by the SEBAL, S-SEBI and SSEB models, for the bare soil, and the respective percentage errors.

DOA	*ETa* – Bare Soil			Error (%) – SEBAL/S-SEBI	Error (%) – SEBAL/SSEB
	SEBAL	S-SEBI	SSEB		
297	1,2*	1,7*	0,7*	41,7	41,7
220	3,3*	4,5*	1,2*	36,4	63,6

*significance level (α) of 5%.

As in this study, Silva et al. (2018) analyzed the ET_a averages calculated by SEBAL from Landsat 8 images, for the municipality Salto Lontra in southwestern Paraná in Brasil, a region composed by agricultural, native vegetation and urban areas, the ET_a ranged between 3.2 and 5, 0 mm/day, and respective relative error, from 4.9 to 37.0%.

The ET_a estimated by the SEBAL, S-SEBI, and SSEB models were tested with the ET_a calculated analytically by multiplying the daily reference evapotranspiration (ET_0) times the cultivation coefficient (k_c) of the banana (Table 10), with k_c equal to 1.10 in the fruiting stage of tropical regions and arid climates (Embrapa, 2020; Texas, 2020). The ET_a obtained through k_c was used as a reference to find the discrepancies with the ET_a estimated by the models.

The day 220 (2006) there was a big difference between the ET_a obtained by the (k_c from that estimated by the models in the orchard area, with percentage errors greater than 30%. The smallest errors occurred on the 297 (2005), which correspond to the dry period (October to December) of the region when rainfall is insufficient, and the water deficit of the plant is high, and the use of irrigation was probably necessary. As stated by Santos (2009), the banana evapotranspiration rate is strongly influenced by the amount of water available in the root zone.

Ruhoff et al. (2012) stated that the results obtained by the SEBAL model indicated that there was a potential to estimate energy fluxes at the surface on clear sky days. The technique is not limited only to irrigated areas, it can be applied in a wide variety of biomes, even if discrepancy daily values for *ET* has occurred, the model must be evaluated not only for the accuracy of the estimated results but also by the ability to provide spatial information in wide areas, which is not possible through data measured *in situ*. Similarly, this same assumption can be extended to the two other algorithms, S-SEBI and SSEB, which are simplified derivations of the SEBAL to be applied in locations where station input data are absent.

Table 10 - Percentage errors of ET_a (mm / day) estimated by the SEBAL, S-SEBI and SSEB models in relation to the observed (Obs.).

DOA	ET_0	*ETa* – Obs.	*ETa* – SEBAL	Error (%)	*ETa* – S-SEBI	Error (%)	*ETa* – SSEB	Error (%)
297/2005	8,7	9,6	9,3	3,1	8,5	11,5	7,3	24,0
220/2006	3,3	3,7	5,8	56,8	6,3	70,3	2.5	32,4

4. Conclusions

The latent heat flux showed a little distinction between the S-SEBI model with respect to SEBAL for the vegetated areas (orchard and Caatinga), while the sensible heat flux exhibited greater variability, which may be related to the more refined processing of the SEBAL.

The evaporative fraction showed good correspondence between S-SEBI and SEBAL, in the vegetated areas. However, for the bare soil, there was a large discrepancy, which may be assigned to the inefficiency of applying S-SEBI in areas without vegetation cover and with low soil moisture content.

The actual daily evapotranspiration (ET_a) calculated by the S-SEBI, was also less discrepant compared to SEBAL in the vegetated areas, but for the bare soil was not. The SSEB underperformed the SEBAl in all areas. Regarding the ET_a estimated by the models with that calculated through the k_c, those showed agreement with the values found during the dry period in which the orchard was irrigated, especially in the SEBAL and S-SEBI cases.

Therefore, among the two algorithms analyzed in relation to SEBAL, S-SEBI performed better to estimate ET_a, with fewer distinctions between the parameters analyzed. However, future studies for the improvement of the SSEB can be done, in order to calibrate it for the semi-arid region and making it a promising tool for qualitative and even quantitative analysis of evapotranspiration, since it consists of an easy application method, which was based on other methods used worldwide.

Acknowledgments

CAPES (Coordination for the Improvement of Higher Education Personnel) for financial support through the granting of a scholarship to the first author and CNPq (National Council for Scientific and Technological Development) for the Research Productivity grant to the second author.

References

Aguiar, R.G., Musis, C.R., Aguiar, L.J.G., Espinosa, M.M., 2018. Energy balance closure in the Southwest Amazon forest site—a statistical approach. Theoretical and Applied Climatology 1, 1-11.

Allen, R.G., Pereira, L.S., Raes, D., Smith, M., 1998. Crop evapotranspiration - Guidelines for computing crop water requirements. FAO, Rome. (Irrigation and Drainage Paper, 56).

Allen, R., tasumi, M., Trezza, R., 2002. SEBAL - Surface Energy Balance Algorithms for Land – Advanced Training and User's Manual – Idaho Implementation, version 1.0.

allen, R.G., Tasumi, M., trezza, R., 2007. Satellite-Based Energy Balance for Mapping Evapotranspiration with Internalized Calibration (METRIC) - Model. Journal of Irrigation and Drainage Engineering 133, 380-394.

Basit, A., Khalil, R.Z., Haque, S., 2018. Application of simplified surface energy balance index (S-SEBI) for crop evapotranspiration using Landsat 8. International Archives of the Photogrammetry, Remote Sensing and Spatial Information Sciences XLII-1, 33-37.

Bastiaanssen, W.G.M., 1995 Regionalization of surface flux densities and moisture indicators in composite terrain: a remote sensing approach under clear skies in Mediterranean climate. Thesis. Landbouwuniversiteit, Wageningen.

Bastiaanssen, W.G.M., Menenti, M., Feddes, R.A., Holtslag, A.A.M., 1998a. A remote sensing surface energy balance algorithm for land (SEBAL) 1. Formulation. Journal of Hydrology 212–213, 198–212.

Bastiaanssen, W.G.M., Pelgrum, H., Wang, J., Ma, Y., Moreno, J.F., Roenrink, G.J., Van Der Wal, T., 1998b. A remote sensing surface energy balance algorithm for land (SEBAL) 2. Validation. Journal of Hydrology 212–213, 213-229.

Bastiaanssen, W.G.M., 2000. SEBAL-based sensible and latent heat fluxes in the irrigated Gediz Basin, Turkey. Journal of Hydrology 229, 87-100.

Bezerra, B.G., Bezerra, J.R.C., Silva, B.B., Santos, C.A.C., 2015a. Surface energy exchange and evapotranspiration from cotton crops under full irrigation conditions in the Rio Grande do Norte State, Brazilian Semi-Arid. Bragantia 74, 120-128.

Bezerra, B.G., Silva, B.B., Santos, A.A.C., Bezerra, J.R.C., 2015b. Actual Evapotranspiration Estimation Using Remote Sensing: Comparison of SEBAL and SSEB Approaches. Advances in Remote Sensing 4, 234-247.

Blain, G.C., Kayano, M.T., Camargo, M.B.P., Lulu, J., 2009. Variabilidade amostral das séries mensais de precipitação pluvial em duas regiões do Brasil: Pelotas-RS e Campinas-SP. Revista Brasileira de Meteorologia 24, 1-11.

Cai, X.L., Sharma, B.R., 2010. Integrating remote sensing, census and weather data for an assessment of rice yield, water consumption and water productivity in the Indo-Gangetic river basin. Agricultural Water Management 97, 309–316.

Cai, X.L., Sharma, B.R., 2009. Remote sensing and census based assessment and scope for improvement of rice and wheat water productivity in the Indo-GangeticBasin. Science in China Series E: Technological Sciences 52, 3300-3308.

Calcagno, G., Mendicino, G., Monacelli, G., Senatore, A., Versace, P., 2007. Distributed estimation of actual evapotranspiration through remote sensing techniques. Water Science and Technology Library 62, 25-148.

Castro, C.A.C., 2002. Interações Trópicos-Extratrópicos na escala de tempo intrasazonal durante o verão austral e seus efeitos na América do Sul. Dissertação (Mestrado). Instituto Nacional de Pesquisas Espaciais, São Paulo.

Danodia, A., Patel, N.R., Chol, C.W., Nikam, B.R., Sehgal, V.K., 2019. Application of S-SEBI model for crop evapotranspiration using Landsat-8 data overparts of North India. Geocarto International 34, 114–131.

Dubreuil, V., Fante, K., Planchon, O., Santa'Anna Neto, J. L., 2018. Os tipos de climas anuais no Brasil: uma aplicação da classificação de Köppen de 1961 a 2015. Confins, 37. doi: https://doi.org/10.4000/confins.15738

EMBRAPA. Empresa Brasileira de Pesquisa Agropecuária, 2020. Coeficientes de cultura para a bananeira para dois métodos de determinação de evapotranspiração de referência. Disponível: https://ainfo.cnptia.embrapa.br/digital/bitstream/CPATSA/30014/1/OPB275.pdf.

Huang, G., Paes, A.T., 2009. Posso usar o teste t de Student quando preciso comparar três ou mais grupos?. Einstein: Educação Continuada em Shuxmaúde 7, 63-64.

Huxman T.E., Wilcox, B.P., Scott, R.L., Snyder, K., Hultine, K., small, E., Breshears, D., Pockman, W.,

JAckson, R.B., 2005. Ecohydrological implications of woody plant encroachment. Ecology 86, 308-319.

Jia, D., Kaishan, S., zongming, W., Bai, Z., Dianwei, L., 2013. Evapotranspiration Estimation Based on MODIS Products and SurfaceEnergy Balance Algorithms for Land (SEBAL) Model in Sanjiang Plain, Northeast China. Chinese Geographical Science 23, 73–91.

Jin, X., ZHU, X., Xue, Y., 2019. Satellite-based analysis of regional evapotranspiration trends in a semi-arid area. International Journal of Remote Sensing 40, 3267–3288.

Kayano, M.T., kousky, V.E., 1996. Tropical circulation variability with emphasis on interannual and intraseasonal time scales. Revista Brasileira de Meteorologia 11, 6-17.

Kazmier, L.J., 1982. Estatística Aplicada à Economia e Administração. McGraw-Hill, São Paulo. (Coleção Schaum).

Knipper, K., Hogue, T., Scott, R., Franz, K., 2017. Evapotranspiration Estimates derived using multi-platform remote sensing in a semiarid region. Remote Sensing 9, 1-22.

Kousky, V.E., Kayano, M.T., 1994. Principal modes of outgoing longwave radiation and 250-mb circulation for the South American sector. Journal of Climate. 7, 1131-1143.

Liou, Y., Kar, S.K., 2014. Evapotranspiration Estimation with Remote Sensing and Various Surface Energy Balance Algorithms—A Review. Energies 7, 2821-2849.

Mendonça, J.C., Sousa, E.F., André, R.G.B., Silva, B.B., Ferreira, N.J., 2012. Estimativa do fluxo do calor sensível utilizando o algoritmo SEBAL e imagens MODIS para a região norte fluminense, RJ. Revista Brasileira de Meteorologia. 27, 85-94.

Najmaddin, P.M., Whelan, M.J., Balzter, H., 2017. Estimating Daily Reference Evapotranspiration in a Semi-Arid Region Using Remote Sensing Data. Remote Sensing 9, 1-20.

Platonov, A., Thenkabail, P.S., Biradar, C.M., Cai, X., Gumma, M., Dheeravath, V., Cohen, Y., Alchanatis, V., Goldshlager, N., Ben-Dor, E., Vithanage, J., Manthrithilake, H., Kendjabaev, S., Isaev, S., 2008. Water Productivity Mapping (WPM) using Landsat ETM+Data for the irrigated croplands of the Syrdarya river basin in Central Asia. Sensors 8, 8156-8180.

Ponzoni, F,J., Pinto, C.T., Lamparelli, R.A.C., Jurandir Junior, Z., Antunes, M.A.H., 2015. Calibração de Sensores Orbitais. Oficina de Textos, São Paulo.

Roerink, G.J., Su, Z., Menenti, M., 2000. A Simple Remote Sensing Algorithm to Estimate the Surface Energy Balance. Physics and Chemistry of the Earth (B) 25, 147-157.

Ruhoff, A.L., Paz, A.R., Collischonn, W., Aragão, L.E.O.C., Rocha, H.R., Malhi, Y.S., 2012. A MODIS-Based energy balance to estimate evapotranspiration for clear-sky days in Brazilian tropical savannas. Remote Sensing 4, 703-725.

Santos, C.A.C., 2009. Estimativa da evapotranspiração real diária através de análises micrometeorológicas e de sensoriamento remoto. Tese. Universidade Federal de Campina Grande, Campina Grande.

Santos, C.A.C., Silva, B.B., 2008. Estimativa da evapotranspiração da bananeira em região semi-árida através do algoritmo S-SEBI. Revista Brasileira de Agrometeorologia 16, 9-20.

Santos, C.A.C., Bezerra, B.G., Silva, B.B., Rao, T.V.R., 2010. Assessment of daily actual evapotranspiration with SEBAL and S-SEBI algorithms in cotton crop. Revista Brasileira de Meteorologia 25, 383-392.

Santos, C.A.C., 2011. Análise das necessidades hídricas da vegetação *tamarisk* através da razão de bowen e do modelo SEBAL. Revista Brasileira de Meteorologia 26, 85-94.

Senay, G.B., Budde, M., Verdin, J.P., Melesse, A.M., 2007. A Coupled Remote Sensing and Simplified Surface Energy Balance Approach to Estimate Actual Evapotranspiration from Irrigated Fields. Sensors 7, 979-1000.

Senay, G.B., Budde, M.E., Verdin, J.P., 2011a. Enhancing the Simplified Surface Energy Balance (SSEB) approach for estimating landscape ET: Validation with the METRIC model. Agricultural Water Management. 98, 606–618.

Senay, G.B., Leake, S., Nagler, P.L., Artan, G., Dickinson, J., Cordova, J.T., Glenn, E.P., 2011b. Estimating basin scale evapotranspiration (ET) by water balance and remote sensing methods. Hydrological Processes 25, 4037–4049.

Silva, D.F., Sousa, A.B., 2013. Detecção de Tendências Climáticas no Estado de Alagoas. Revista Brasileira de Geografia Física 6, 442-455.

Silva, B.B., Mercante, E., Boas, M.A.V., Wrublack, S.C., Oldon, L.V., 2018. Satellite-based ET estimation using Landsat 8 imsampaioages and SEBAL model. Revista Ciência Agronômica 49, 221-227.

Sobrino, J.A., Gómez, M., Jiménez Muñoz, J.C., Olioso, A., Chehbouni, G., 2005. A simple algorithm to estimate evapotranspiration from DAIS data: Application to the DAISEX Campaigns. Journal of Hydrology 315, 117-125.

Su, Z., 2002. The Surface Energy Balance System (SEBS) for estimation of turbulent heat fluxes. Hydrology and Earth System Sciences 6, 85–99.

Sun, M., Dong, Q., Jiao, M., Zhao, X., Gao, X., Wu, P., Wang, A., 2018. Estimation of Actual

Evapotranspiration in a Semiarid Region Based on GRACE Gravity Satellite Data — A Case Study in Loess Plateau. Remote Sensing 10, 1-15.

Trezza, R., 2002. Evapotranspiration using a satellite-based Surface energy balance with standardized ground control. Thesis. Utah State University, Logan.

Wang, K., Li, Z., Cribb, M., 2006. Estimation of evaporative fraction from a combination of day and night land surface temperatures and IVDN: a new method to determine the Priestley–Taylor parameter. Remote Sensing of Environment 102, 293–305.

Weligepolage, K., 2005. Estimation of spatial and temporal distribution of evapotranspiration by satellite remote sensing – a case study in Hupselse Beek, The Netherlands. Dissertation. International Institute for Geo-information Science and Earth Observation, Waganingen.

Yang, X., Ren, L., Jiao, D., Yong, B., jiang, S., Song, S., 2013. Estimation of daily actual evapotranspiration from ETM+ and MODIS data of the headwaters of the west Liaohe basin in the semiarid regions of china. Journal of Hydrologic Engineering 18, 1530-1538.

Yebra, M., Dijk, A.V., Leuning, R., Huete, A., Guerschman, J.P., 2013. Evaluation of optical remote sensing to estimate actual evapotranspiration and canopy conductance. Remote Sensing of Environment 129, 250–261.

Zahira, S., Abderrahmame, H., Mederbal, K., Frederic, D., 2009. Mapping latent heat flux in the western forest covered regions of Algeria Using Remote Sensing Data and a Spatialized Model. Remote Sensing 1, 795-817.